Subscale-Model and Full-Scale Engine Mixed-Flow Exhaust System Performance Comparison

A. P. Kuchar*
General Electric Company, Cincinnati, Ohio
and
R. Chamberlin†
NASA Lewis Research Center, Cleveland, Ohio

A full-scale engine test of the NASA/General Electric Company (GE) Energy Efficient Engine (E^3) was conducted to demonstrate the E^3 engine concept and evaluate its performance. The test program, performed at the GE outdoor engine test facilities in Peebles, Ohio, included a detailed evaluation of the total pressure and temperature profiles at the exit of the mixed-flow exhaust system to determine its mixing effectiveness. Subscale model tests of the same mixed-flow exhaust system had been previously conducted at FluiDyne Engineering Corporation in Minneapolis as part of the GE E^3 mixer aerodynamic technology development program. The scale-model and full-scale engine nozzle exit survey data and the calculated mixing effectiveness are compared and discussed. The results indicate the effectiveness of the full-scale engine mixing to be 5% higher than that of the scale model as a result of a geometric difference and higher turbulence levels in the engine exhaust flowfield.

Nomenclature

A = flow area
C_P = specific heat at constant pressure
D_{MP} = exhaust duct diameter at the mixing plane
H_L = mixer annular height perpendicular to streamlines
H_{MP} = flow passage annular height at the mixer trailing edge and perpendicular to streamlines
K_4 = mixing effectiveness determined from nozzle exit P_T and T_T survey data
L = mixing length from the mixer trailing edge to the nozzle exit plane
P_0 = ambient pressure
P_T = total pressure
ΔP_T = mixer aerodynamic pressure loss determined from scale model thrust data
ΔSFC = specific fuel consumption benefit relative to confluent flow with no mixing
T_T = total temperature
V = velocity
W = weight flow
$\Delta\theta$ = circumferential travel of nozzle exit survey rakes

Subscripts

5 = core charging station
8 = nozzle exit station
14 = fan charging station
16 = fan conditions at mixing plane
56 = core conditions at mixing plane

Presented as Paper 84-0283 at the AIAA 22nd Aerospace Sciences Meeting, Reno, NV, Jan. 9-12, 1984; received May 24, 1984; revision received June 7, 1985.

*Manager, GE37 Exhaust System Aero Design, Advanced Engineering Technologies Department. Member AIAA.

†Facility Manager, 10×10 Supersonic Wind Tunnel and Flight Programs, Aero Propulsion Facilities and Experiments Division.

Introduction

IN 1976, NASA began the Aircraft Energy Efficiency (ACEE) Program. The ACEE Program is directed toward developing new technology for energy-efficient aircraft and propulsion systems. The General Electric Company (GE) has participated in several elements of the ACEE Program, including the Energy Efficient Engine (E^3) Program under a contract managed by the NASA Lewis Research Center. The goal of the E^3 program was to develop the component technology needed to provide significant fuel savings on future engines that will also have lower operating costs, reduced noise, and reduced emissions. To help achieve this goal, the GE E^3 design incorporates a long-duct, mixed-flow exhaust system. As part of the E^3 design effort, GE conducted a three-phase scale-model static performance test program of the mixed-flow exhaust system at FluiDyne Engineering Corporation in Minneapolis. The test program was conducted to establish a technology data base from which an advanced technology, high-performance mixer could be designed.

The development of the E^3 engine component technology culminated in a full-scale engine test. This engine, designated the integrated core/low spool (ICLS) engine, was tested at the GE outdoor engine test facility in Peebles, Ohio, in April/June 1983. The ICLS nacelle was a nonflight, boilerplate type of design that simulated the internal mixer and exhaust system flowpath. The same mixer/exhaust system flowpath was also tested during the scale-model component development program. Test data were recorded that allowed a determination of the mixing effectiveness of the ICLS mixer in a manner identical to the data analyses performed in the scale-model program. The results from the scale-model development tests have been previously reported in Refs. 1 and 2. This paper presents a detailed comparison of the mixing effectiveness results between the scale-model and full-scale ICLS engine tests.

Test Hardware Description

The mixer configuration in the ICLS test vehicle was selected from the results of the scale-model development program. A flowpath cross section and description of the ICLS mixer aerodynamic design is presented in Fig. 1. The selected mixer had 12 lobes with scalloped, radial sidewalls. The penetration H_L/H_{MP} was established from a performance tradeoff of mixing effectiveness vs mixer pressure loss based on results from the scale-model tests. The mixing length L/D_{MP} was determined from an optimization study that accounted for internal performance (mixing effectiveness and internal pressure loss), nozzle weight, nacelle external drag, and aircraft weight (flutter) penalty.

An overall cross section of the ICLS engine test configuration is shown in Fig. 2 and the scale-model cross section in Fig. 3. The test models were 12% scale and simulated the ICLS internal exhaust system flowpath aft of the fan frame/outlet guide vanes and aft of the low-pressure turbine discharge. This simulation included the fan duct, core duct, turbine frame, mixer, nozzle centerbody, pylon, engine aft mount struts, and exhaust nozzle. The model was thermally insulated to prevent conduction heat transfer between the hot core hardware and the cold fan hardware upstream of the mixer. Several features of the ICLS test vehicle were not simulated on the scale model. These features are shown in Fig. 2 and include: an instrumentation leadout strut located downstream of the mixer and in line with a fan lobe, a fan air scoop (to provide active clearance control air for the turbines), a strut on the engine bottom centerline for the slave gearbox drive train, and a center vent tube protruding from the exhaust centerbody.

Instrumentation

Both the scale-model and full-scale engine were instrumented with total pressure and temperature rakes located upstream of the mixer at the exhaust system entrance (charging station) to determine fan and core flow conditions. Nozzle exit survey rakes were installed in both test programs to determine the nozzle exit total pressure and temperature profiles. One total pressure rake and two total temperature rakes were orientated in the scale model as shown in Fig. 4. The rakes were indexed during a test point to traverse over a circumferential span of 15 deg for sector A and 18 deg for sector B in 3 deg increments. The ICLS exit survey rake orientations are shown in Fig. 5. For the ICLS tests, four rakes were installed with total pressure and total temperature elements on each rake located at the same relative radial locations as the scale model. These rakes were also indexed circumferentially during a test point in 3 deg increments over a circumferential span of 30 deg, twice that of the scale model. Thus, two rakes traversed from the center of a fan lobe to the center of the next fan lobe.

In addition to the charging station and nozzle exit rake instrumentation, both the ICLS and scale-model hardware incorporated static pressure instrumentation in the exhaust system on the nozzle centerbody, outer exhaust duct, and inner fan duct wall.

Test Description

The scale-model test was conducted at FluiDyne Engineering Corporation's Medicine Lake Laboratory in Minneapolis. In addition to the exit survey data, model thrust was measured in a two-temperature flow, static thrust stand to determine the performance of the various mixer configurations. The scale-model performance results have been previously reported in Ref. 2; this paper deals only with the exit survey data and analysis directly comparable to the ICLS survey data. The ICLS engine test was conducted on site IV D at the GE outdoor engine test facilities in Peebles, Ohio. Testing of the overall engine performance and acoustics was performed and nozzle exit surveys made.

For the scale-model tests, exit survey data were recorded at three fan and core stream pressures and temperatures that covered the expected range of important ICLS engine sea level static operation. In addition, scale-model survey data were recorded at a simulated maximum cruise altitude operating condition. Since the scale-model test was conducted more than 2 years prior to the ICLS tests, estimates of the engine operating conditions had to be made. When the final turbomachinery component operating maps were updated and the engine was tested, the actual operating conditions differed somewhat from the scale-model test. A comparison of the fan and core pressure and temperature ratios for the ICLS and scale-model tests is presented in Fig. 6. The effect of these differences is discussed in the following section.

Results and Discussion

In the scale-model mixer development program, the mixed-flow exhaust system performance parameters of interest were the mixing effectiveness and the mixer pressure loss. Mixing effectiveness is defined as the ratio of actual thrust gain due to mixing to the theoretical thrust gain for fully mixed flow as originally developed by Frost,[3] and expressed in the following equation:

$$K_4\text{, mixing effectiveness} = \frac{\text{actual thrust-(fan thrust + core thrust)}}{\text{theoretical 100\% mixed thrust-(fan thrust + core thrust)}} \times 100$$

Mixer pressure loss is defined as the total, mass-weighted fan and core stream pressure loss due to the mixer and includes the aerodynamic friction on the surface of the lobes, the pressure

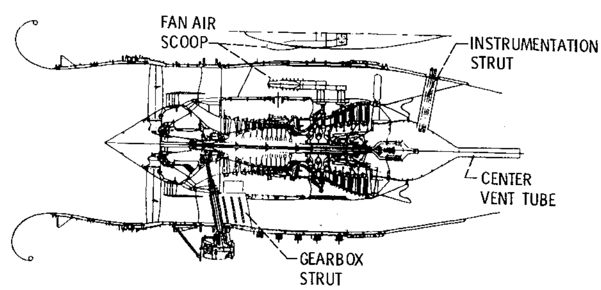

Fig. 2 ICLS engine cross section.

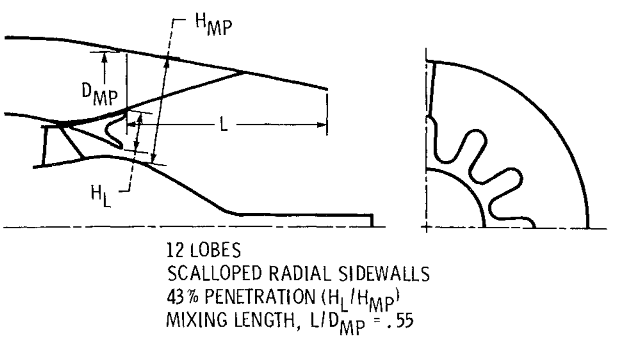

Fig. 1 Mixer geometry description.

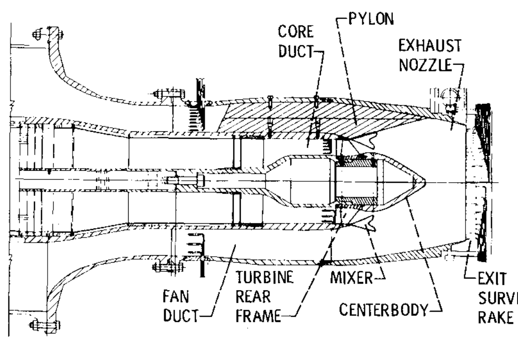

Fig. 3 Scale-model cross section.

loss due to the velocity difference of the two streams, and the secondary flow/turning losses of the air within the lobes. Both of these performance parameters were evaluated in the scale-model program. Mixing effectiveness was calculated by two independent methods using the measured thrust and the nozzle exit surveys. The thrust data were used to calculate mixing effectiveness for each mixer by comparing the increase in thrust coefficient from cold-flow to hot-flow conditions with the theoretical thrust coefficient increase for 100% mixing at the model test conditions. The exit survey rake data were integrated to determine the mixing effectiveness by calculating both a fully mixed temperature and an actual mixed temperature. The ratio of these temperatures was used in combination with the measured upstream fan and core temperatures and airflows to determine a mixing effectiveness as shown in the following equations:

K_4 rake survey =

$$\left\{\left(\frac{T_{T\text{actual mixed}}}{T_{T100\%\text{ mixed}}}\right)^{1/2}_{\text{rake survey}}(W_{14}+W_5)(T_{T100\%\text{ meas.}})^{1/2} - (W_{14}(T_{T14})^{1/2}+W_5(T_{T5})^{1/2})\right\}$$

$$\div\left\{(W_{14}+W_5)(T_{T100\%\text{ meas.}})^{1/2}-(W_{14}(T_{T14})^{1/2}+W_5(T_{T5})^{1/2})\right\}$$

where:

$$T_{T\text{actual mixed}} = \left(\int_{\text{exit}} W_i(T_{Ti})^{1/2} \Big/ \int_{\text{exit}} W_i\right)^2$$

$$T_{T100\%\text{ mixed}} = \int_{\text{exit}} W_i T_{Ti} \Big/ \int_{\text{exit}} W_i$$

$$T_{T100\%\text{ meas.}} = \frac{W_{14}C_{P14}T_{T14}+W_5C_{P5}T_{T5}}{W_{14}C_{P14}+W_5C_{P5}}$$

Mixer aerodynamic pressure loss was determined by comparing the cold-flow thrust coefficient of a confluent reference configuration with the cold-flow thrust coefficient of the lobed mixer configuration. The cold-flow thrust coefficient difference was then converted to a pressure loss that is attributed to the mixer. Since the ICLS engine obviously cannot be run under cold-flow conditions, the only quantitative performance parameter that could be directly compared between the scale-model and ICLS tests is the mixing effectiveness as determined from an integration of the nozzle exit survey data. This comparison is presented in Fig. 7 vs the nozzle pressure ratio. Also shown in the figure is the mixing effectiveness from the scale-model exit survey integration at the maximum cruise design point. The two sets of data indicate that the ICLS mixing effectiveness is approximately 8% higher than the scale model.

A detailed analysis, beginning with a comparison of the nozzle exit temperature profiles, was subsequently conducted to determine the reasons for the increased mixing effectiveness. Figure 8 compares the envelope encompassing all of the survey data from a scale-model test point with the envelope from a corresponding ICLS survey test point. The temperatures are presented in nondimensionalized form relative to the fan and core discharge temperatures. The nondimensionalized temperatures are plotted vs nozzle area distribution where a value of zero is at the nozzle centerline and a value of 1.0 is at the nozzle exit diameter. Detailed profiles have been presented in Ref. 4.

The comparison in Fig. 8 revealed three differences between the two sets of data. First, the hot-flow spike observed in the scale-model data near the nozzle centerline is significantly reduced in the ICLS data. This reduction was not totally unexpected. The large center vent tube shown in Figs. 1 and 2 was not simulated on the scale model, and analytical studies using a mixing analysis compter program indicate that the turbulence generated along such a surface will, in general,

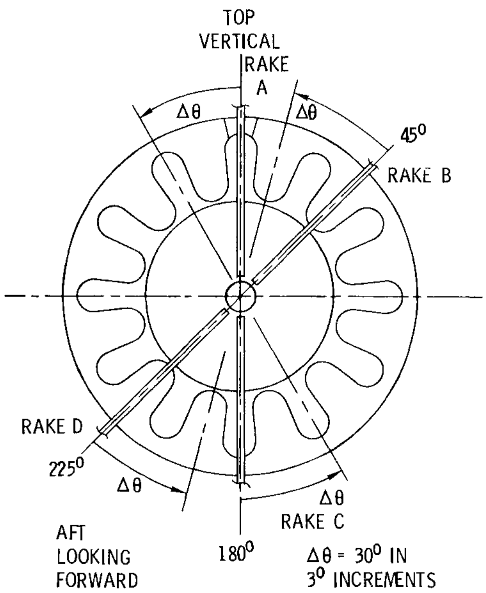

Fig. 5 ICLS survey rakes.

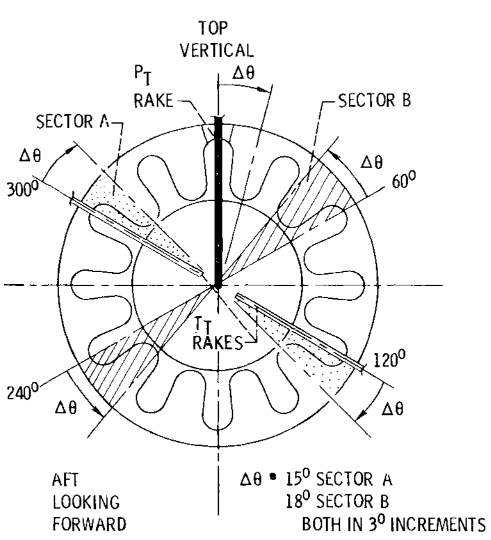

Fig. 4 Scale-model survey rakes.

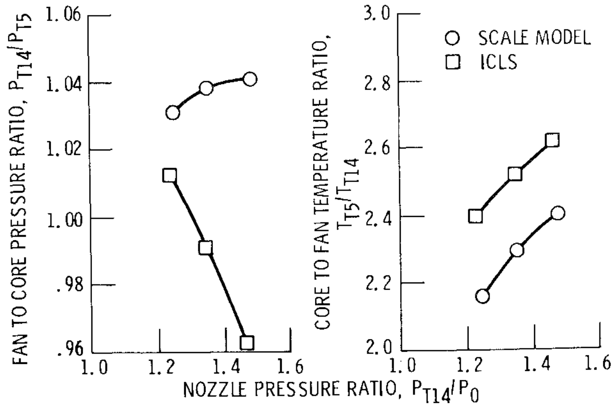

Fig. 6 Comparison of test conditions.

enhance mixing. The center vent tube, being an extension of the centerbody, would have had the same effect. To estimate the impact of this difference on mixing effectiveness, the temperature level of the spike measured on the ICLS was superimposed on the scale-model profiles and the scale-model mixing effectiveness was recalculated. From this analysis, it was determined that the reduction in the scale-model hot-flow spike would have increased mixing effectiveness by approximately 3%.

The second major difference between the scale-model and ICLS profiles is the apparent improved circumferential mixing on the ICLS. The comparison in Fig. 8 shows less temperature variation in the ICLS data, on the average, at any given radial (percent nozzle area) position. Although it has not been supported analytically, this improvement is concluded to be the result of higher turbulence levels in the ICLS flowfield relative to the scale model. This will be discussed further in subsequent paragraphs.

The third major difference is that the ICLS hot-flow penetrates radially outward approximately 10% more than the scale model. It has been concluded that this higher flow penetration is due to a higher core-to-fan velocity ratio at the mixing plane achieved on the ICLS. The higher velocity ratio, which will also be discussed further in subsequent paragraphs, apparently increased the mixing effectiveness by 2-3%.

When the scale-model mixing effectiveness data were originally evaluated, the variation in mixing effectiveness shown in Fig. 7, particularly at the low-pressure ratio, was concluded to be the result of data scatter. Thus, any trends were considered insignificant. Several of the E^3 mixer configurations evaluated in the initial scale-model test phase were also simulated on a TF34 engine and tested in 1980 in one of the NASA Lewis Propulsion System Laboratory altitude test chambers as part of the Propulsion Engine Technology (PET) program. Results of these tests, reported in Ref. 5, seemed to support the conclusion that the mixing effectiveness was essentially independent of the operating conditions. However, the similarity between the ICLS and scale-model data trends shown in Fig. 7 prompted a reassessment of all the existing E^3 and TF34 PET data to determine if the operating conditions had an affect on the mixing effectiveness. It was ultimately concluded from this reassessment that the velocity ratio of the two streams at the mixing plane has a second-order effect on mixing effectiveness. A one-dimensional velocity for each stream was calculated from the measured airflow, total pressure and temperature shown in Fig. 6, and the calculated flow area of each stream at the mixing plane. The correlation, shown in Fig. 9, is intuitive; a higher velocity difference should promote mixing by virtue of the increased shear forces and energy exchange between the two streams.

A significant difference in the relative positions of the individual test data points results by using the velocity ratio as the independent parameter vs using the nozzle pressure ratio. The two sets of data are now 5-6% different rather than 8%, and the equivalent nozzle pressure ratio points at the ICLS maximum power condition ($P_{T14}/P_0 = 1.47$) are at opposite ends of the curves. This significant difference in velocity ratio between the ICLS and the scale model at the maximum power condition is due to differences in the fan-to-core pressure and temperature ratios as shown in Fig. 6. The fan-to-core pressure ratio, P_{T14}/P_{T5}, in the scale model was 1.04, whereas on the ICLS it was 0.96. Part of the reason for the lower value on the ICLS was due to the much larger blockage of the ICLS survey rakes compared to the scale model. The survey rake blockage reduced the nozzle effective exit area, which subsequently decreased the engine bypass ratio. During the ICLS performance tests without the rakes installed, the pressure ratio increased to 0.996. The rest of the difference in the pressure ratio was due to the final, actual operating characteristics of the ICLS test vehicle compared to the estimate that had been made 2 years earlier for the scale-model test. Thus, the lower fan-to-core pressure ratio for the ICLS

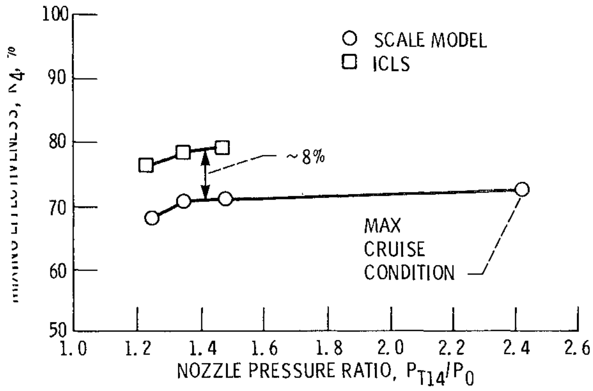

Fig. 7 Calculated mixing effectiveness determined from nozzle exit survey data.

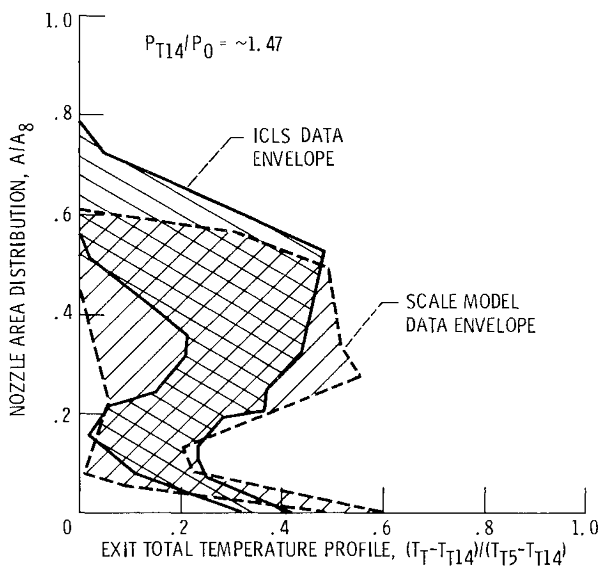

Fig. 8 Comparison of ICLS and scale-model temperature profile envelopes.

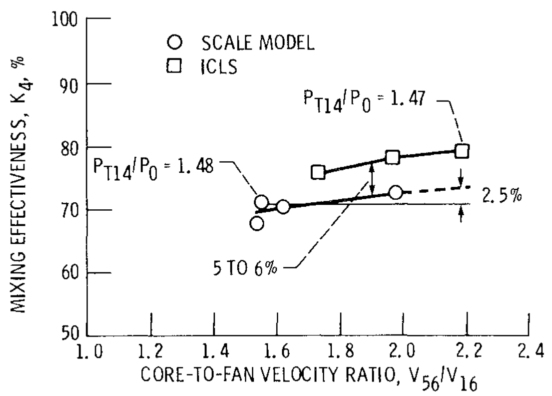

Fig. 9 Mixing effectiveness dependency on mixing plane velocity ratio.

survey tests effectively decreased the bypass ratio and increased the velocity ratio relative to the scale model. Additionally, the ICLS core-to-fan temperature ratio T_{T5}/T_{T14}, was higher than the scale model (2.6 vs 2.4), which also increased the velocity ratio. Based upon the correlation in Fig. 9, if the scale model at $P_{T14}/P_0 = 1.48$ were run at the same velocity ratio as the ICLS, it would have shown an increase in mixing effectiveness of approximately 2.5%.

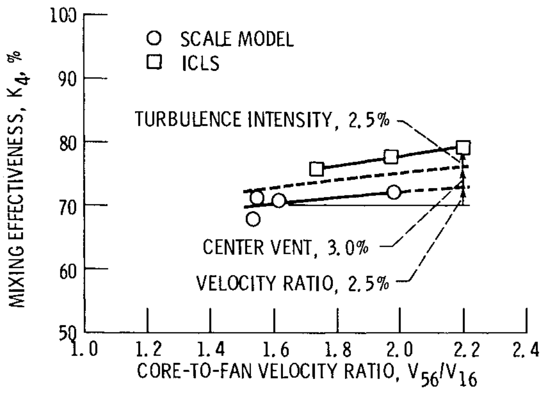

Fig. 10 Model-to-full-scale mixing effectiveness stackup.

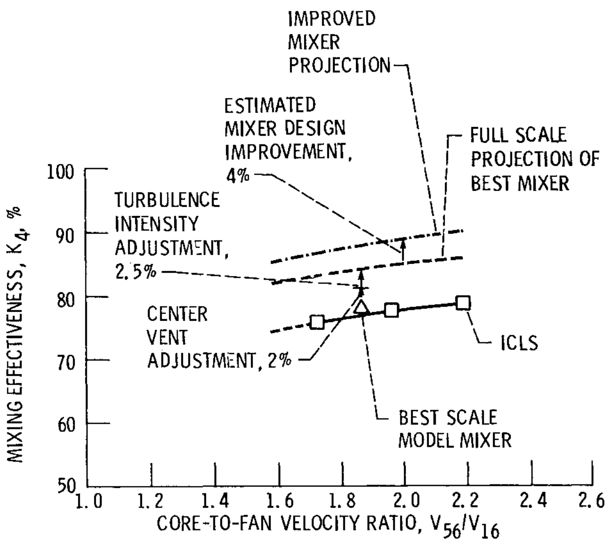

Fig. 11 Mixing effectiveness projection.

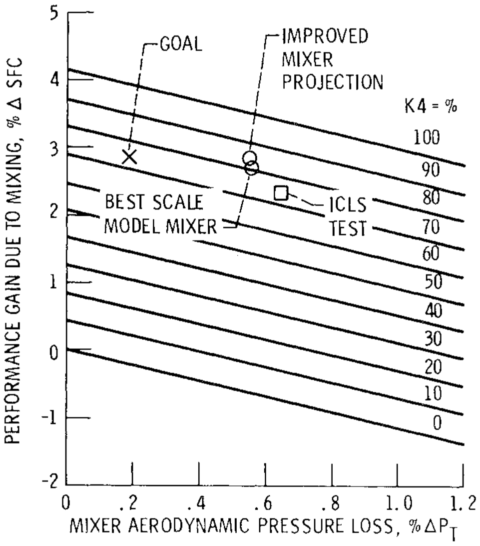

Fig. 12 Mixer performance gain summmary at Mach 0.8/35,000 ft maximum cruise.

A stackup explaining the differences in the mixing effectiveness shown in Fig. 7 was formulated from these analyses and is summarized in Fig. 10. First, an increase in mixing effectiveness of 2.5% is due to the higher velocity ratio. The higher velocity ratio achieved on the ICLS test was concluded to be the reason for the increased hot-flow penetration observed in the exit temperature profiles. Second, an increase in the mixing effectiveness of 3% is due to the presence of the center vent tube on ICLS. Since the magnitude of the hot-flow spike near the nozzle centerline did not change with the pressure ratio on either the scale-model or ICLS tests, the calculated 3% increase would be essentially constant. Finally, the remaining 2.5% increase is concluded to be due to a higher level of turbulence likely in an actual engine exhaust flowfield vs a scale model. Increased turbulence levels should be expected in full-scale engine flows due to the upstream rotating turbomachinery in both streams, the combustion process in the core stream, and the acoustic/noise level in the two streams. Industry research[6,7] has shown that acoustic sources imposed on two mixing streams of different temperatures can enhance the degree of mixing. While this phenomenon has not been analytically investigated to quantify the effects on mixing, it has been surmised that a 2-3% increase in mixing effectiveness from this turbulence associated phenomenon is not unreasonable and appears to represent a valid adjustment to scale-model data. This phenomenon is the probable cause of the increased circumferential mixing observed in the temperature profiles of the ICLS data. Although not reported in Ref. 5, the TF34 PET tests also indicated mixing effectiveness levels slightly higher than the scale model. Thus, while scale-model testing has been concluded to be a valid mixer aerodynamic development tool, model performance results may, in fact, be slightly conservative because of the lower tubulence levels inherent with a scale-model flowfield.

The ICLS mixer configuration represented an interim design in the E^3 program because of the need to make an engine configuration selection prior to the last phase of the scale-model tests. The phase III model tests reported in Ref. 2 evaluated configurations with further improvements in mixer/exhaust system performance. The best mixer configuration tested in the scale-model program had a mixing effectiveness of 79.2% at a velocity ratio of 1.87. Two adjustments to these data are valid based on the ICLS data and the foregoing analysis. It can be expected that the scale-model mixing effectiveness will increase due to better mixing at the nozzle centerline because of the center vent tube. In this case, the scale-model mixer had a smaller hot-flow spike than the ICLS scale-model mixer, and the gain in mixing effectiveness calculated by superimposing the ICLS hot spike on the scale model was 2%. Adding the 2.5% model-to-full-scale flowfield turbulence intensity adjustment results in a mixing effectiveness of 83.7%. This value, combined with the scale-model velocity ratio and the slope of the ICLS mixing effectiveness vs the velocity ratio characteristics, was used to estimate the full-scale mixing effectiveness characteristic for the best mixer tested in the scale-model program, as presented in Fig. 11. As a result of the scale-model test development program, it was concluded that, with additional work, an improvement from 79% to 85% in mixing effectiveness of the best scale-model mixer could be achieved through some combination of lobe shape change, increased penetration, and increased number of lobes. Part of the 6% improvement would have come from an elimination of the hot-flow spike at the nozzle centerline. Since this has already been accounted for as shown in Fig. 11 (2%), it can be concluded that further improvements in the mixer design that result in a 4% improvement in mixing effectiveness are achievable. Adding this to the full-scale projection of the best mixer tested results in the improved mixer projection curve in Fig. 11.

Several comments with regard to the mixing effectiveness-to-velocity ratio relationship are appropriate. It is expected that the slope of the mixing effectiveness vs velocity ratio characteristic is not a unique thermodynamic effect and could vary with the configuration and engine cycle. Thus, the two dashed line projections in Fig. 11, in reality, may differ in slope from the curves shown. Additionally, the fact that the mixing effectiveness apparently increases with the velocity ratio should not be construed as a design goal to maximize the velocity ratio. While this is a positive benefit in terms of mixing effectiveness, the pressure loss due to the thermodynamic mixing process will increase with higher velocity ratios. Thus, in an ultimate design, the velocity ratio as a design variable must be evaluated as a tradeoff between improved mixing effectiveness and increased thermodynamic mixing pressure loss.

Results of the ICLS tests in terms of mixing effectiveness were favorable from two aspects. First, the mixing effectiveness achieved was more than 5% higher than the scale model at equivalent operating conditions, due to the flowfield turbulence level differences and the center vent geometry difference. Second, the test data established the effect of mixing plane velocity ratio on performance and the need for its inclusion in engine cycle deck modeling of mixer performance. Results were also used to project the estimated mixer performance for an improved mixer design derived for the phase III scale-model test.

The purpose of incorporating a mixed-flow exhaust system is to improve engine fuel consumption. The performance benefits in terms of ΔSFC due to the mixer is shown in Fig. 12 for a GE E^3 cycle at altitude cruise conditions. The ΔSFC improvement is defined as the improvement in performance relative to confluent flow with no mixing, as if the fan and core streams were independently expanded to ambient conditions through the long duct exhaust system. This specific definition of ΔSFC allows a determination of the net performance gain (ΔSFC) due to just the mixer component in terms of its two specific performance parameters (mixing effectiveness and mixer pressure loss) at a specific engine operating condition. Since the mixer aerodynamic pressure loss could not be determined from the ICLS tests, the scale-model derived pressure loss for both the ICLS mixer configuration and the best phase III scale-model mixer configuration was used. This approach was considered valid because variations in the fan-to-core operating conditions in the model test had shown to have no measurable effect on the mixer pressure loss. The pressure loss values are 0.66 and 0.57% for the ICLS and best scale-model mixers, respectively. At a Mach 0.8/35,000 ft maximum cruise condition, the velocity ratio for the GE E^3 cycle is approximately 1.6 for optimum performance. At this velocity ratio, the mixing effectiveness values for the ICLS configuration, the best scale-model configuration adjusted to full scale and the improved mixer projection as shown in Fig. 11 are 74, 81, and 85%, respectively. These three values combined with the appropriate mixer pressure loss are shown on Fig. 12 to define the corresponding ΔSFC improvement. The prime aerodynamic design objective is to develop mixer configurations that have performance characteristics falling in the upper left-hand corner of this figure. The lobed mixer configuration developed in this program resulted in higher pressure losses than originally anticipated, but also higher levels of mixing effectiveness, which together yielded an SFC improvement the same as the goal level. Further increases in mixing effectiveness or reductions in mixer pressure loss may still be possible with improved designs or alternate mixer concepts.

Conclusions

A detailed, comparative analysis of total pressure and temperature surveys measured at the nozzle exit plane of the scale-model and full-scale ICLS engine mixed-flow exhaust systems provided valuable insight to the aerothermodynamic behavior of mixed-flow systems. In particular, the analysis yielded important conclusions with regard to the validity of scale-model testing and the understanding of the effects of mixed-flow exhaust system geometric and aerodynamic parameters on mixing effectiveness.

Integration of the exit survey data showed that the mixing effectiveness of the full-scale ICLS engine mixer/exhaust system was approximately 8% higher than the subscale model at the same nozzle pressure ratio. The higher mixing effectiveness of the ICLS exhaust system was attributed to three effects:

1) The fan and core stream total pressure and temperature ratios in the ICLS engine differed from the scale model, resulting in a higher average core-to-fan velocity ratio at the mixing plane than the scale model. The higher velocity ratio increased the aerodynamic penetration of the hot-flow stream and resulted in a higher mixing effectiveness.

2) The addition of the center vent tube on the ICLS engine provided more surface area to generate additional turbulence. The added turbulence promoted further mixing and reduced the size of the hot-flow spike near the nozzle centerline.

3) It is presumed that the engine turbomachinery created a higher turbulence level than existed in the subscale model. This resulted in less circumferential temperature variation in the engine and, therefore, better mixing.

Although a higher mixing plane velocity ratio appears to increase mixing, it has also been concluded that:

1) The dependency of mixing on the velocity ratio observed in these tests probably varies with different geometries and different engine cycles.

2) Higher velocity ratios do not necessarily mean higher net performance; the thermodynamic pressure loss due to the mixing process will also increase, suggesting that an optimum velocity ratio exists which balances mixing effectiveness, mixing pressure loss, and possibly engine turbomachinery cycle matching.

The improvement in circumferential mixing due to the presumed higher turbulence levels in the ICLS engine exhaust flow is surmised to be a reasonable increase and represents a valid adjustment of the model to a full-scale engine that can be applied for most high-performance lobed mixer designs. This conclusion, combined with the overall data analysis and the previous experience in the TF34 PET Programs,[5] lends credibility to the use of scale models to develop the aerothermodynamic design of mixed-flow exhaust systems.

References

[1]Kuchar, A. P. and Chamberlin, R., "Scale Model Performance Test Investigation of Exhaust System Mixers for an Energy Efficient Engine (E^3) Propulsion System," AIAA Paper 80-0229, Jan. 1980.

[2]Kuchar, A. P. and Chamberlin, R., "Scale Model Performance Test Investigation of Mixed Flow Exhaust Systems for an Energy Efficient Engine (E^3) Propulsion System," AIAA Paper 83-0541, Jan. 1983.

[3]Frost, T. H., "Practical Bypass Mixing Streams for Fan Jet Aero Engines," *Aeronautical Quarterly,* May 1966.

[4]Kuchar, A. P. and Chamberlin, R., "Comparison of Full Scale Engine and Subscale Model Performance of a Mixed Flow Exhaust System for an Energy Efficient Engine (E^3) Propulsion System," AIAA Paper 84-0283, Jan. 1984.

[5]Cullom, R. R., Bobula, G. A., and Burkardt, L. A., "Mixing Effectiveness Test of an Exhaust Gas Mixer in a High Bypass Turbofan at Altitude," NASA TM 82663, July, 1981.

[6]Oh, Y. H. and Bushnell, D. M., "Influence of External Disturbances and Compressibility on Free Turbulent Mixing," NASA SP-347, 1975, Sec. 10.

[7]Marinet, M. F. and Binder, G., "Structure des Jets Pulsants," *Journal de Mécanique,* Vol. 18, NO. 2, 1979.